JETIR.ORG ISSN: 2349-5162 | ESTD Year : 2014 | Monthly Issue
JOURNAL OF EMERGING TECHNOLOGIES AND INNOVATIVE RESEARCH (JETIR)
An International Scholarly Open Access, Peer-reviewed, Refereed Journal

Influence of interplanetary coronal mass ejection associated with shocks and sheath regions on the terrestrial environment

F. Mustajab[1], Badruddin[2]

[1] Scholar (WOS-A), [2]Professor[1]Centre for Theoretical Physics (CTP), Jamia Millia Islamia, New Delhi 110025, India

[2]Astronomy Department, Faculty of Science, King Abdulaziz University, Jeddah 21589, Saudi Arabia

Abstract: Coronal mass ejection (CME) is a huge mass of plasma and magnetic field originated from the Sun. These CME propagates into the interplanetary space with different features and structures and is identified as interplanetary coronal mass ejection (ICMEs). When ICMEs become faster than proceeding solar wind a shock wave develops. The turbulent region between shock and ICMEs is known as the sheath region. Some of them reach the Earth and create different types of disturbances. To understand and describe the proper ties of the different structures, producing disturbances of different magnitude and nature, we use the spacecraft measurements of ICMEs with different magnetic properties propagating into interplanetary space and generating disturbances. We use their different plasma and field properties to investigate for different interplanetary parameters influencing the geomagnetic behaviour by different coronal mass ejections associated features.

***Index Terms*- Coronal mass ejections, solar wind, shocks, sheath regions, geomagnetic disturbances.**

Introduction

Interplanetary coronal mass ejections from the Sun are considered as the main source of geomagnetic disturbances ([31],[12],[14]), the form of geomagnetic storms or solar energetic particles (SEPs) (see, *e.g.*, [4], [11], [12] and [30] references therein). While all the ICMEs do not create the geomagnetic disturbance ([23], [24], [1]). A subset of ICMEs with plasma/field properties is called ICMEs with shocks. When an ICME is sufficiently faster than the preceding solar wind, a shock wave develops ahead of the ICME. The turbulent region between the shock and the ICME is called the sheath region [18]. ICMEs can be identified by many criteria, although a universal ICME signature is not yet determined ([8], [33], [28]). However, typical signatures of ICMEs, when compared to the ambient solar wind, can include one or more of the following: strong and smooth magnetic field, low proton temperature and density, low plasma β, smooth and large rotation of the magnetic field, declining speed, enhanced helium abundance, counter streaming suprathermal electron beams, enhanced ion-charge states, and others (see, *e.g.*, [4], [2], [19], [21], [7], [10], [29], [34], [35] and [6]).

ICMEs and their sheaths and shocks are all interesting structures from space weather disturbances in the heliosphere and planetary environments. ICME-driven shock waves can accelerate charged particles to high energies. Sheaths and ICMEs drive practically all intense geospace storms at the Earth, and they can also dramatically affect planetary radiation environments and atmospheres.

The ICME occurrence rate can be associated with the solar-cycle phase and generally the solar activity. It is higher during solar maximum and lowers during solar minimum (see, *e.g.*, [20]). However, the correlation is not simple, as, for example, during the last solar cycle, the ICME rate demonstrated a short decline in 1999, while the solar cycle was rising, and remained high during the years 2004 – 2005 although the solar cycle was declining, as indicated by Richardson and Cane [27].

Fast ICMEs can create shocks in the interplanetary medium. These shocks are often identified by *in-situ* data as a sudden rise of plasma speed, magnetic field, proton density, and proton temperature. When a shock is created and driven by the ICME, we call the area between theshock and the ICME a "sheath". In the sheath, the solar wind is compressed, which leads to an increased magnetic field with large amplitude fluctuations. These fluctuations often produce high negative values of the *z*-component of the magnetic field (B_z), which are likely to cause strong effects in the Earth's magnetosphere (*e.g.* [5], [35]). There are many studies concerning catalogues and statistical properties of ICMEs (*e.g.* [3], [14], [21], [32], [15], [16], [28]). In other studies, the properties of ICMEs and their sheaths are compared ([9], [22], [13] and [25]).

We also are discussing the current understanding of space weather consequences of these large-scale solar wind structures, including effects,

properties, and consequences of the sheaths and ICMEs. View the ICMEs and their sheath regions, associated with shocks based on observations from Richardson and Cane catalogue, and we discuss their role in driving space weather disturbances. It will also be interesting to compare recovery characteristics of ICME associated with shocks and no shocks and sheath with shocks and no shocks.

1. ICMEs/sheath during the Time Period 1996 to 2008 (solar cycle 23)

In this study we have identified 325 ICMEs events, many driving interplanetary shocks are identified by their signatures, for the time period 1996 to 2008, which includes Solar Cycle 23. The data set came from the OMNI near-Earth database at a resolution of one minute and included solar-wind and magnetic-field data, which are: magnetic-field strength, their RMS values, down-dusk electric field, solar-wind speed, proton density, and plasma β including geomagnetic index Dst and ap. Out of 325 sheath events, only 34% are not associated with shocks while 66% are shock associated.

Table 1: Distribution of geomagnetic disturbances of different intensity (in numbers and in percentage)(Q, W, M, and I) during the passage of the sheath

Group	Total events	Q(-30nT<Dst<-1nT)	W(-50nT<Dst<-30nT)	M(-100nT<Dst<-50nT)	I(Dst<-100nT)
Shock associated with sheath/ICMEs	213	42(20%)	35(16%)	70(33%)	66(31%)
No shock associated with sheath/ICMEs	112	41(37%)	32(28%)	31(28%)	8(7%)

To identify them we used an approach similar to that of [17]. In this study, we used the following signatures to define the boundaries of the ICMEs: i) strong magnetic-field magnitude, ii) magnetic-field magnitude with decreased variance compared with the ambient solar wind, iii) low proton temperature, iv) low proton density, v) low plasma β, vi) smooth and large rotation of the magnetic field, vii) declining speed, and viii) driven shock. We visually inspected the data and thoroughly examined the instances where the signatures were applied. It is not necessary for all of the above-mentioned signatures to apply in every ICME. However, at least one of i), ii), or vi) combined with at least twoof iii), iv), v), vii), or viii) must apply. We placed the start and end boundaries on apparent changes or discontinuities of the above-mentionedsolar-wind parameters.

In the cases where a shock, temporally close, prior to the identified ICME was present, we regarded it as an ICME-driven shock. The shock is identified by an abrupt and simultaneous rise in all of the following parameters of the solar wind: magnetic-field strength, speed, and proton density. We have observed that in 66% of our cases an ICME-driven shocks are present.

We acknowledge that these sheaths, due to the lack of shocks, probably do not have the same properties as the sheaths with shocks. We placed the start boundary of the sheath at the time that any of the different phases ((i) less than 6 hours, G1, (ii) between 6 and 10 hours; G2 and (iii) more than 10 hours; G3) properties started to apparently increase. We chose two published ICME catalogs to compare with our study: the first by [28], [15], and [16] updated online until 2010.

2. Superposed epoch analysis for ICMEs/Sheaths when associated with shocks or not

We use superposed epoch analysis on 325events during 1996 to 2008 (or solar cycle) for the plasma/field parameters (magnetic field; B, their rms values; rmsB, magnetic field component; Bz, down-dusk electric field; Ey, proton density; N, speed; V and plasma beta; β with two geomagnetic parameters Dst and ap indexes. For the study of geo-affectivity we observe the (Dst)min for all individual events during the passage of sheath region and categorized into four groups on the bases of Dst as quiet 'Q- (-30nT<Dst<-1nT)', weak 'W- (-50nT<Dst<- 30nT)', moderate 'M- (-100nT<Dst<-50nT)' and Intense 'I-(Dst<-100nT)' and tabulated them into table 1. From table 1, we found when the shocks are not associated with sheath 65% produce quiet and weak geomagnetic disturbances and only 35% are strong while in the case when shocks are associated with sheath only 36% are quiet and weak. Most of the shock-associated streams produce strong geomagnetic storms (about 64%).

Fig. 1(a, b, c and d) represents the superposed epoch analysis. Table 2 shows the respective results of the analysis in the form of amplitudes with standard error of the mean for the ICMEs/sheath associated with shocks/no shocks. In light of the table 2, we found ICMEs with Sheath when associated with shocks have higher amplitudes in comparison to those not associated with shocks and also study the time profile of all plasma/ field parameters have their Sudden Storm Commencements (SSC) i.e.; amplitude peak found lag/lead to disturbances (Dst indexes peach) is less for shock associated ICMEs and sheath in compare of not associated shock events. We categorize the ICME/Sheath events into three convenient groups on the basis of the difference between start times of ICMEs and start time of sheath, for example, (i) less than 6hours (G1), (ii) between 6 and 10 hours (G2) and (iii) more than 10 hours (G3). Fig. (a, b and c) and fig.3 (a, b and c) show the result of superposed epoch analysis for groups G1, G2 and G3 without shocks and with shocks respectively. Table 3a and 3b represent the amplitudes time profile and standard error of the mean for all plasma/field parameters and indexes for G1, G2 and G3 groups without shocks and with shocks respectively. With reference to tables 3a and 3b, we found that the events in group G1, all the parameters have their higher amplitudes in comparison of both groups and when associated with shocks have higher amplitudes than no shocks associated events. i.e, when ICMEs start as sheaths start at the same time (or after a few hours) amplitudes of all the parameters are enhanced in comparison to those events having a far difference. When events having ICEMs start time as sheath start time associated with shocks are more geoeffective in comparison to those not associated with shocks.

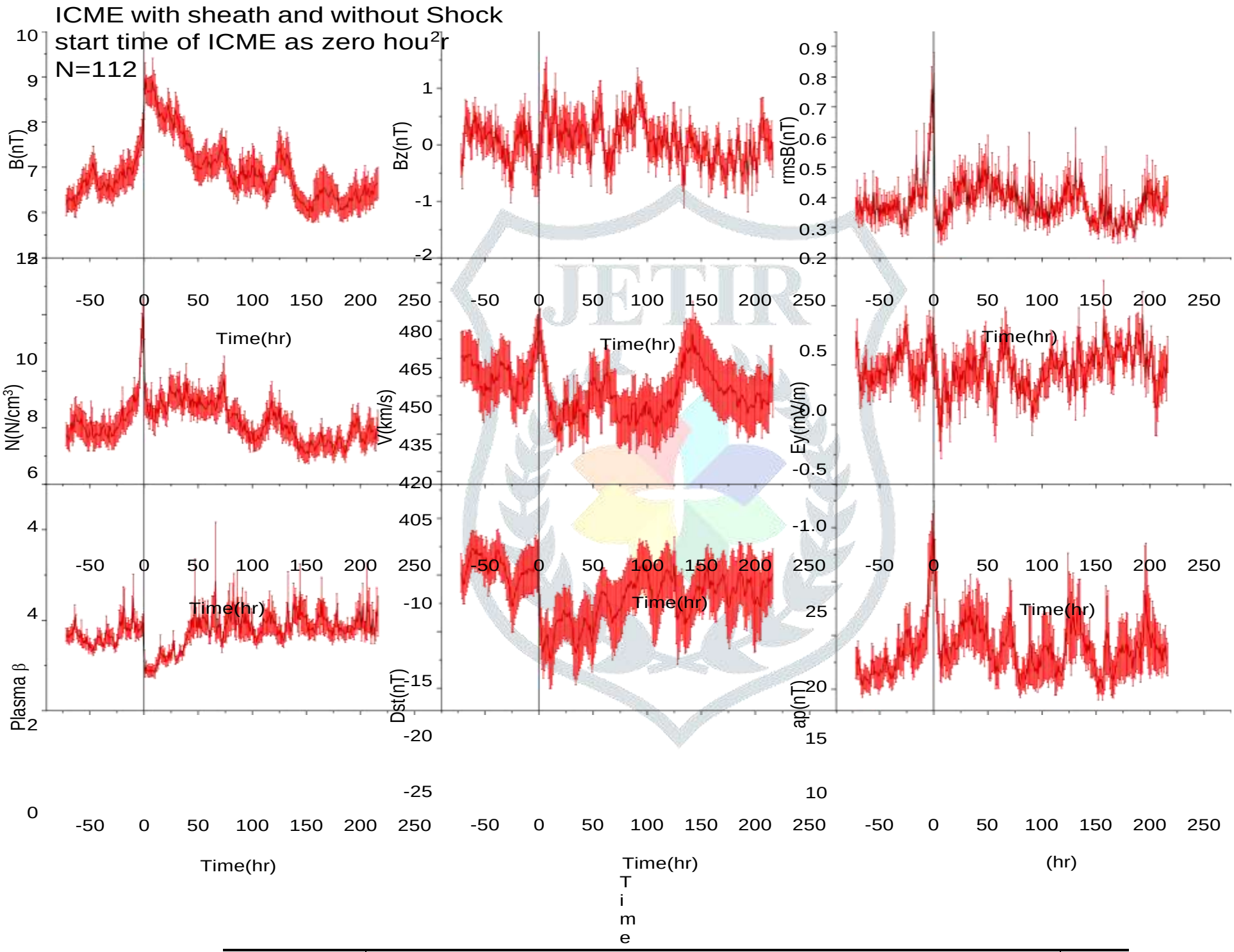
ICME with sheath and without Shock
start time of ICME as zero hour
N=112
B(nT)
Bz(nT)
rmsB(nT)
N(N/cm3)
V(km/s)
Ey(mV/m)
Plasma β
Dst(nT)
ap(nT)
Time(hr)
Time(hr)
Time(hr)
Time(hr)
Time(hr)
Time(hr)
Time(hr)
Time(hr)
Time(hr)
Time

Fig.1a. Superposed epoch analysis results of hourly data for various parameters with respect to the arrival of ICMEs without sheath without shock.

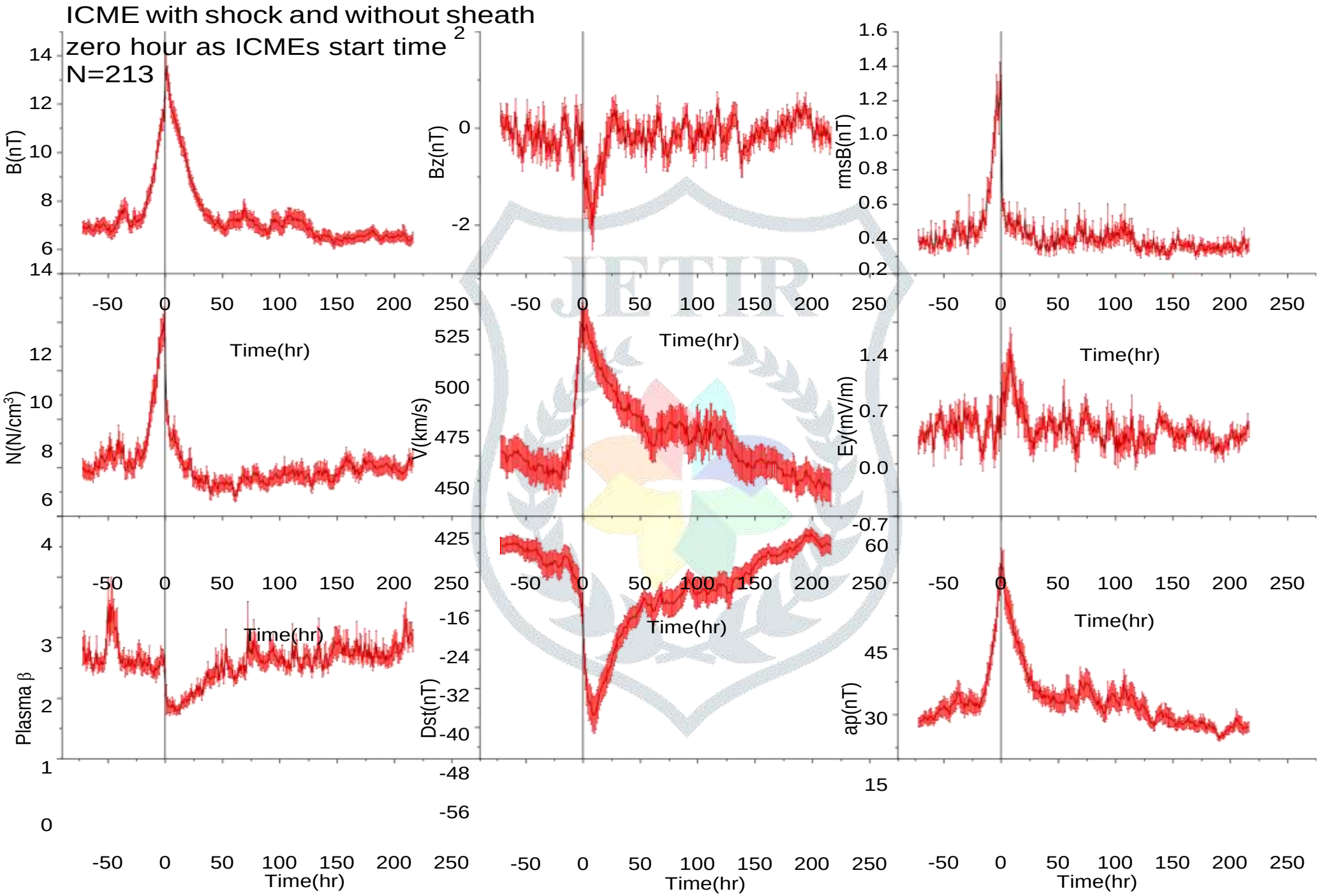
ICME with shock and without sheath
zero hour as ICMEs start time
N=213
B(nT)
Bz(nT)
rmsB(nT)
N(N/cm3)
V(km/s)
Ey(mV/m)
Plasma β
Dst(nT)
ap(nT)
Time(hr)

Fig.1b. Superposed epoch analysis results of hourly data for various parameters with respect to the arrival of ICMEs without sheath with shock

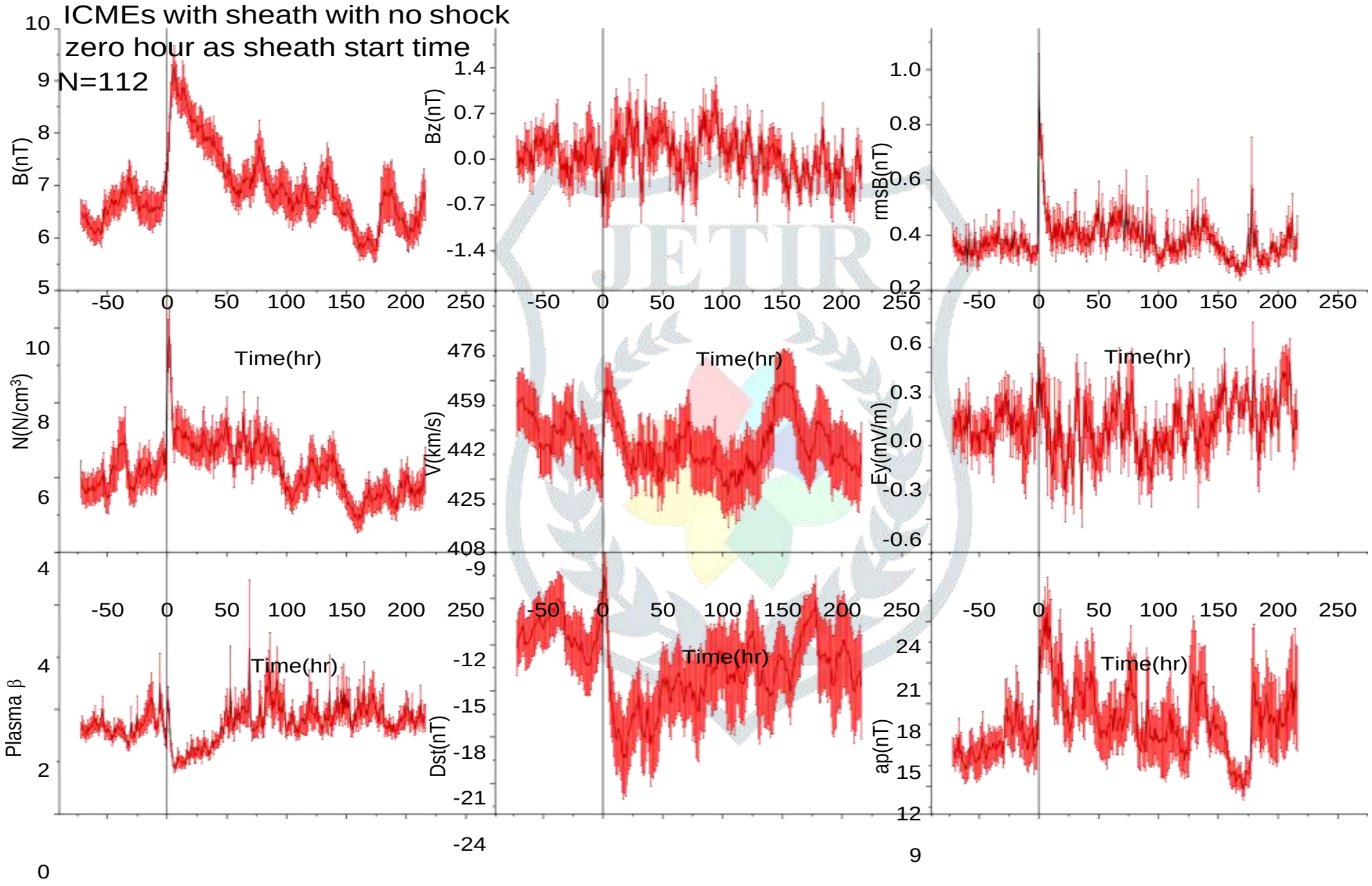
ICMEs with sheath with no shock
zero hour as sheath start time
N=112
B(nT)
Bz(nT)
rmsB(nT)
N(N/cm3)
V(km/s)
-Ey(mV/m)
Plasma β
Dst(nT)
ap(nT)
Time(hr)

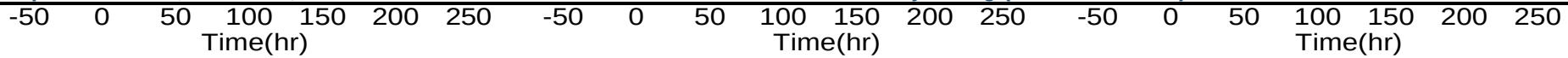

Fig.1c. Superposed epoch analysis results of hourly data for various parameters with respect to the arrival of ICMEs with sheath without shock

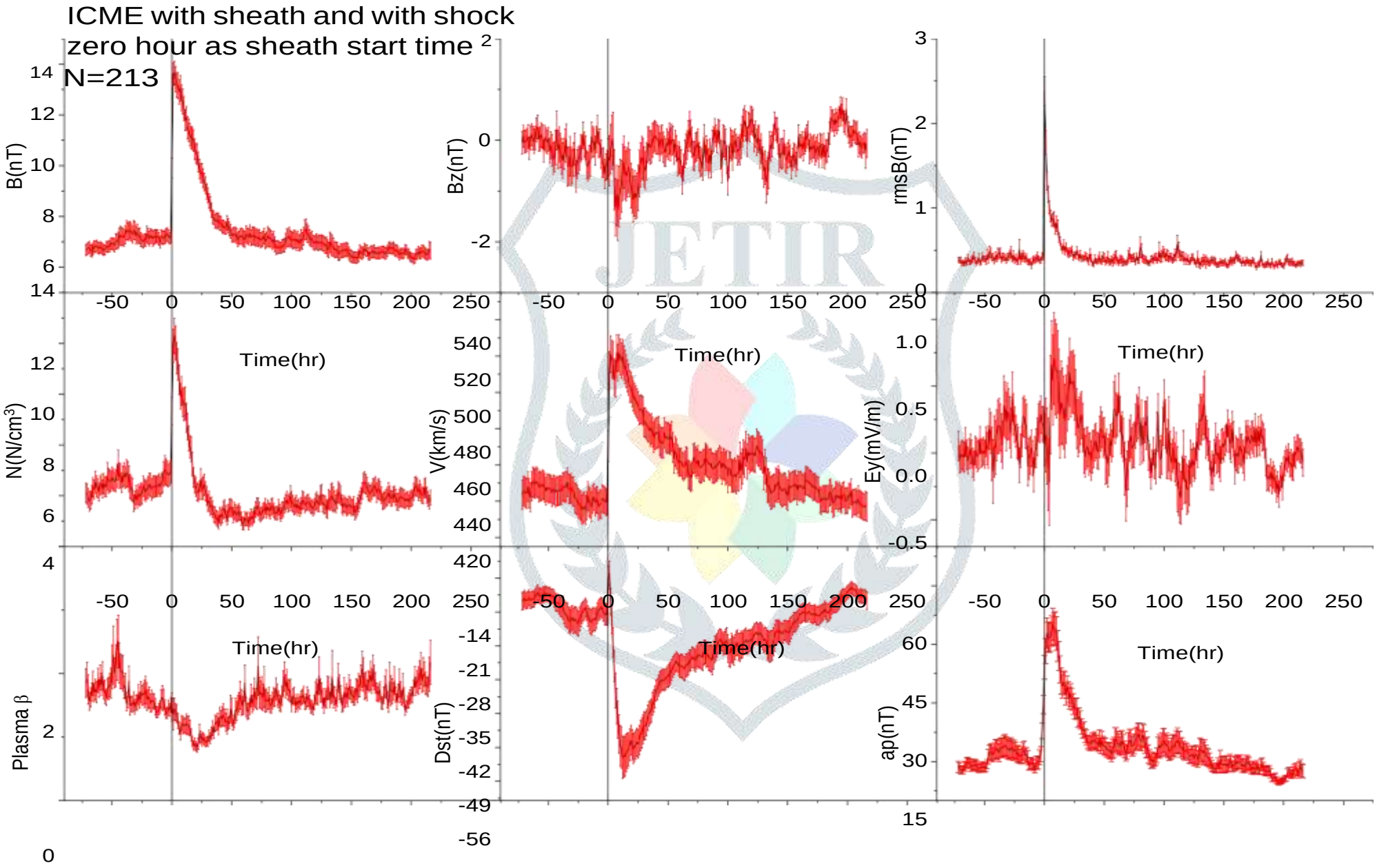
ICME with sheath and with shock
zero hour as sheath start time
N=213
B(nT)
Bz(nT)
rmsB(nT)
N(N/cm3)
V(km/s)
Ey(mV/m)
Plasma β
Dst(nT)
ap(nT)
Time(hr)

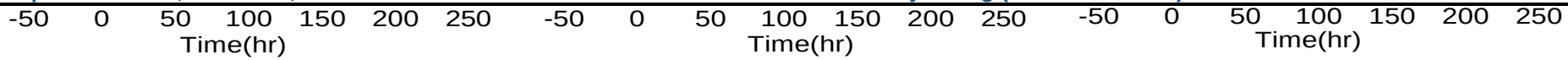

Fig.1d. Superposed epoch analysis results of hourly data for various parameters with respect to the arrival of ICMEs with a sheath with shock.

Table 2: Amplitudes with standard error of mean and time obtained from the superposed results for various parameters for the group sheath start time and ICMEs start time associated with shocks and not associated with shock.

Group	B(nT)			Bz(nT)			rmsB(nT)			N(N/cm³)			V(km/s)			Ey(mV/m)			Plasma Betta			Dst(nT)			Ap(nT)		
	Hr	Am	Se(±)	Hr	Am	Se(±)	Hr	Am	Se(±)	Hr	Am	Se(±)	Hr	Am	Se(±)	Hr	Am	Se(±)	Hr	Am	Se(±)	Hr	Am	Se(±)	Hr	Am	Se(±)
ICME without shock	1	8.96	0.345	-3	-0.54	0.38	0	0.81	0.068	-1	9.90	0.72	0	460.53	8.65	-4	0.26	0.20	1	0.83	0.08	11	-22.38	2.63	0	24.61	2.82
ICME with Shock	1	13.54	0.54	8	-2.11	0.48	0	1.26	0.82	-1	11.96	0.67	-1	515.75	9.88	8	1.06	0.28	7	0.84	0.11	9	-53.35	3.79	0	48.82	3.87
Sheath without shock	6	9.24	0.43	1	-0.71	0.31	0	0.95	0.10	2	9.76	0.81	3	456.58	8.34	1	0.33	0.15	6	0.87	0.08	17	-22.36	2.88	7	21.58	2.6
Sheath with shock	1	13.60	0.45	8	-1.37	0.60	0	2.38	0.17	2	12.30	0.70	7	521.76	10.10	8	0.71	0.34	21	0.83	0.07	12	-51.05	4.36	7	50.12	4.14

Table 3a: Amplitudes with standard error of mean and time obtained from the superposed results for various parameters for the group ICME with sheath (sheath start time as zero hour) associated without shocks for the different phase (G-1; gap between sheath start time and ICME start time <6hour, G-2; gap is in between 6 to 10hour and G-3; when gap >10hours) of solar cycle.

Group	B(nT)			Bz(nT)			rmsB(nT)			N(N/cm³)			V(km/s)			Ey(mV/m)			Plasma Betta			Dst(nT)			Ap(nT)		
Sheath without shock	Hr	Am	Se(±)	Hr	Am	Se(±)	Hr	Am	Se(±)	Hr	Am	Se(±)	Hr	Am	Se(±)	Hr	Am	Se(±)	Hr	Am	Se(±)	Hr	Am	Se(±)	Hr	Am	Se(±)
G-1	1	9.52	0.88	1	-1.07	0.52	0	0.89	0.11	2	10.46	1.00	3	443.13	11.13	1	0.47	0.23	7	0.62	0.05	7	-23.32	4.02	45	21.88	5.88
G-2	6	9.93	1.64	4	-0.81	0.99	0	1.04	0.41	8	9.54	2.14	7	484.91	21.25	31	0.69	0.49	14	0.68	0.18	32	-24.67	6.36	7	25.67	5.38
G-3	3	8.97	0.73	16	-1.26	0.76	0	1.10	0.16	2	9.07	1.90	14	476.90	16.37	16	0.69	0.38	6	1.00	0.13	68	-25.97	5.74	9	27.26	6.26

Table 3b: Amplitudes with standard error of mean and time obtained from the superposed results for various parameters for the group ICME with sheath (sheath start time as zero hour) associated with shocks for the different phase (G-1; gap between sheath start time and ICME start time <6hour, G-2; gap is in between 6 to 10hour and G-3; when gap >10hours) of solar cycle.

Group	B(nT)			Bz(nT)			rmsB(nT)			N(N/cm³)			V(km/s)			Ey(mV/m)			Plasma Betta			Dst(nT)			Ap(nT)		
Sheath with shock	Hr	Am	Se(±)	Hr	Am	Se(±)	Hr	Am	Se(±)	Hr	Am	Se(±)	Hr	Am	Se(±)	Hr	Am	Se(±)	Hr	Am	Se(±)	Hr	Am	Se(±)	Hr	Am	Se(±)
G-1	5	14.73	1.16	11	-3.15	0.99	0	2.75	0.42	2	12.40	1.27	2	549.02	21.30	11	212	0.68	29	0.82	0.09	12	-62.03	10.36	3	59.51	8.33
G-2	2	13.54	0.72	26	-2.06	0.85	0	2.43	0.27	2	14.28	1.30	8	526.21	17.58	26	1.02	0.45	20	0.66	0.08	17	-49.42	5.01	7	47.57	6.33
G-3	3	13.56	0.81	6	-1.59	0.79	0	2.14	0.23	5	13.63	1.17	10	512.80	14.67	6	0.85	0.42	21	0.7	0.08	21	-50.86	4.91	2	47.91	6.39

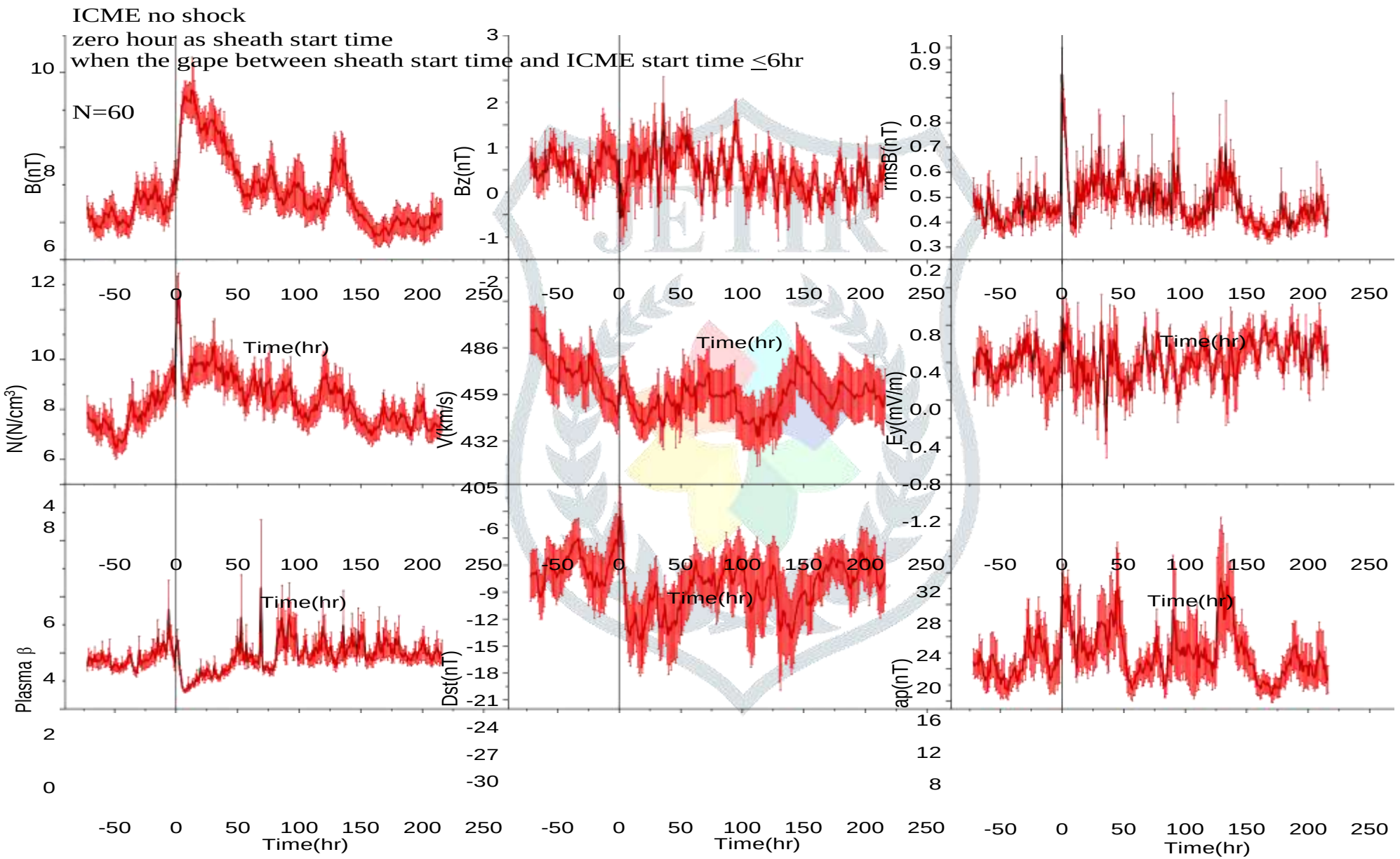
ICME no shock
zero hour as sheath start time
when the gape between sheath start time and ICME start time ≤6hr
N=60
B(nT)
Bz(nT)
rmsB(nT)
N(N/cm3)
V(km/s)
Ey(mV/m)
Plasma β
Dst(nT)
ap(nT)
Time(hr)

Fig.2a. Superposed epoch analysis results of hourly data for various parameters with respect to the arrival of the sheath when the start time of ICMEs and sheath start time gap ≤6 hr without shock.

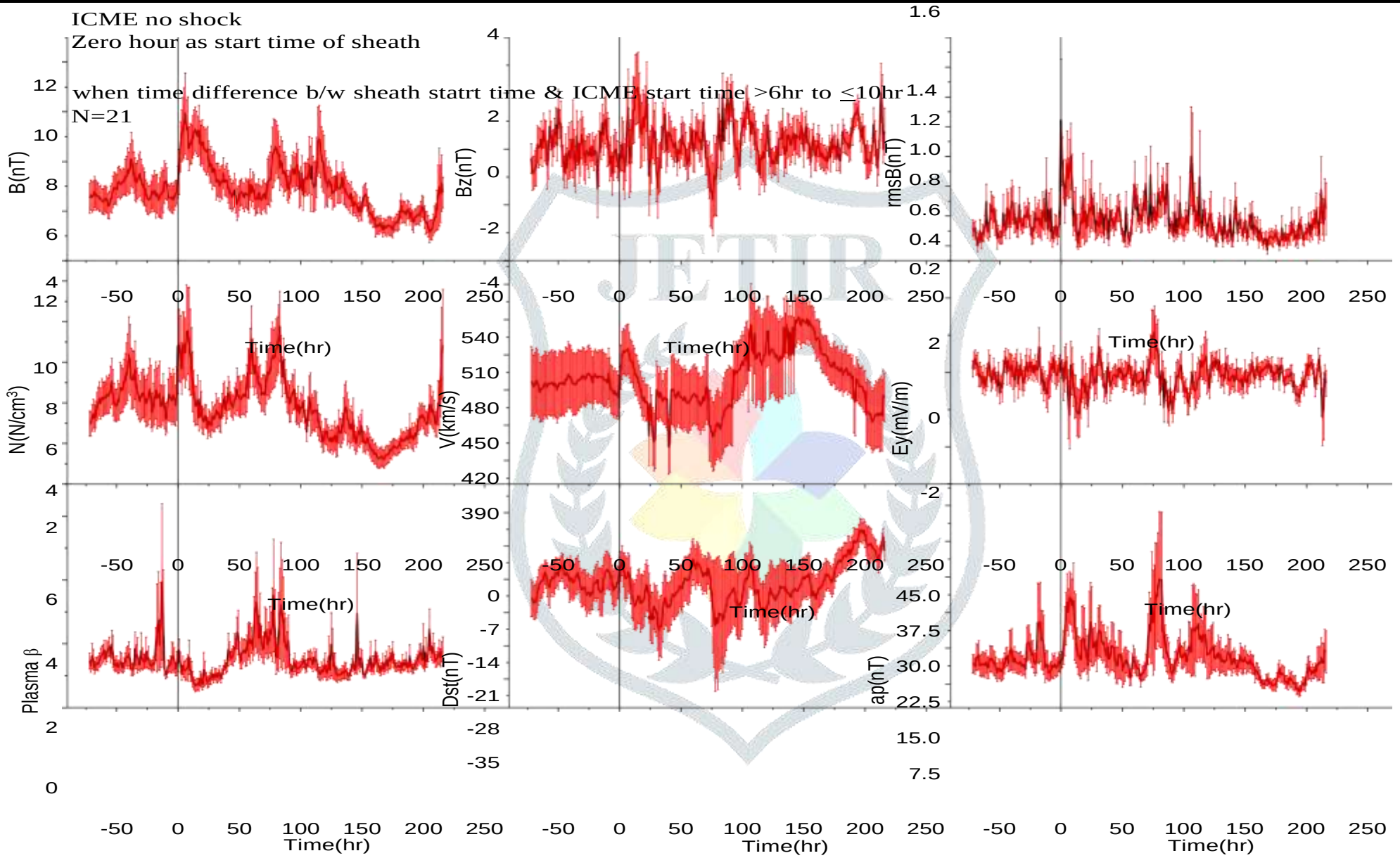
ICME no shock
Zero hour as start time of sheath
when time difference b/w sheath statrt time & ICME start time >6hr to ≤10hr
N=21
B(nT)
Bz(nT)
rmsB(nT)
N(N/cm³)
V(km/s)
Ey(mV/m)
Plasma β
Dst(nT)
ap(nT)
Time(hr)

Fig.2b. Superposed epoch analysis results of hourly data for various parameters with respect to the arrival of the sheath when start time of ICMEs and sheath start time gap >6hr and≤10hr without shock.

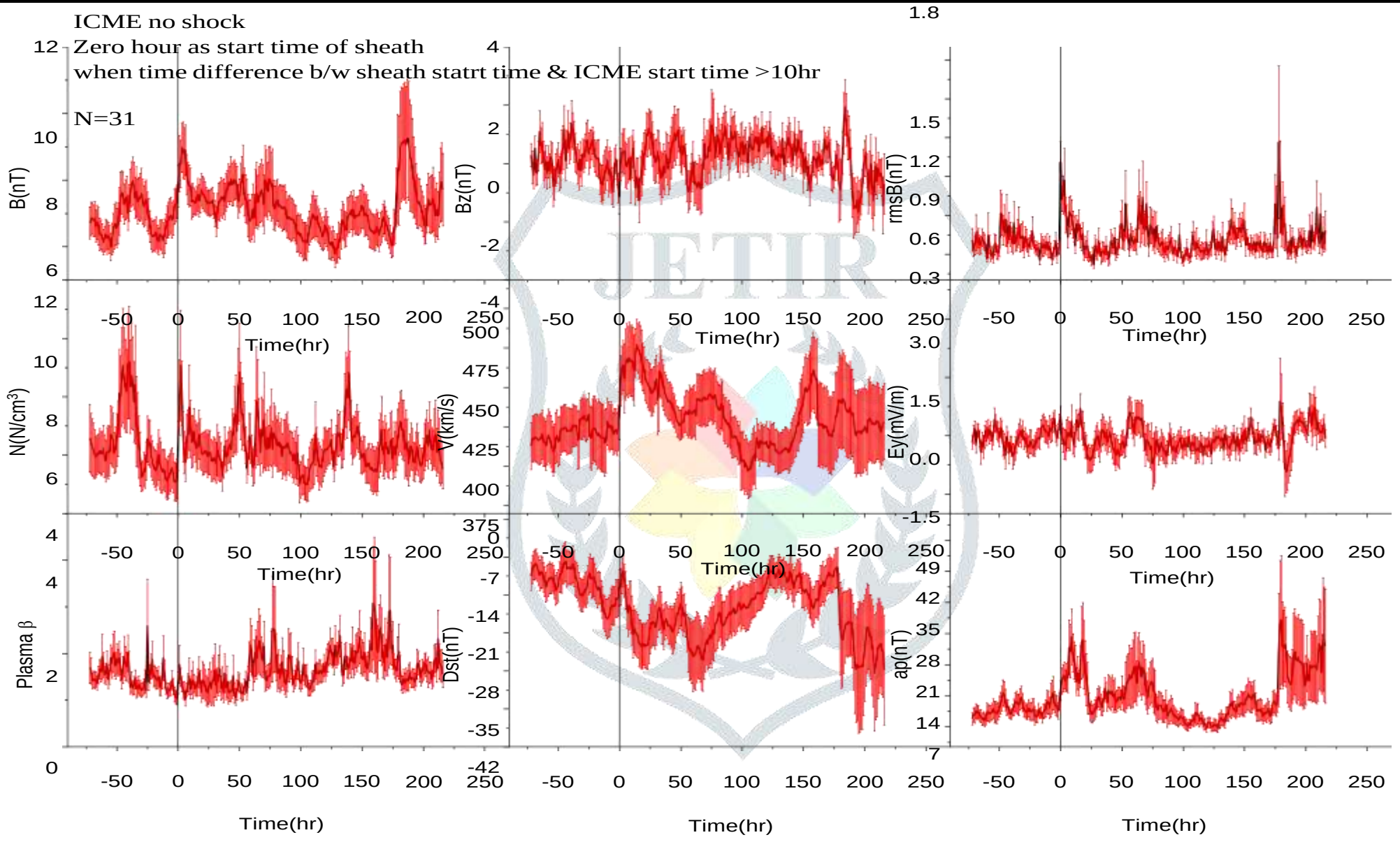

Fig.2c. Superposed epoch analysis results of hourly data for various parameters with respect to the arrival of the sheath when start time of ICMEs and sheath start time gap ≥10hr without shock.

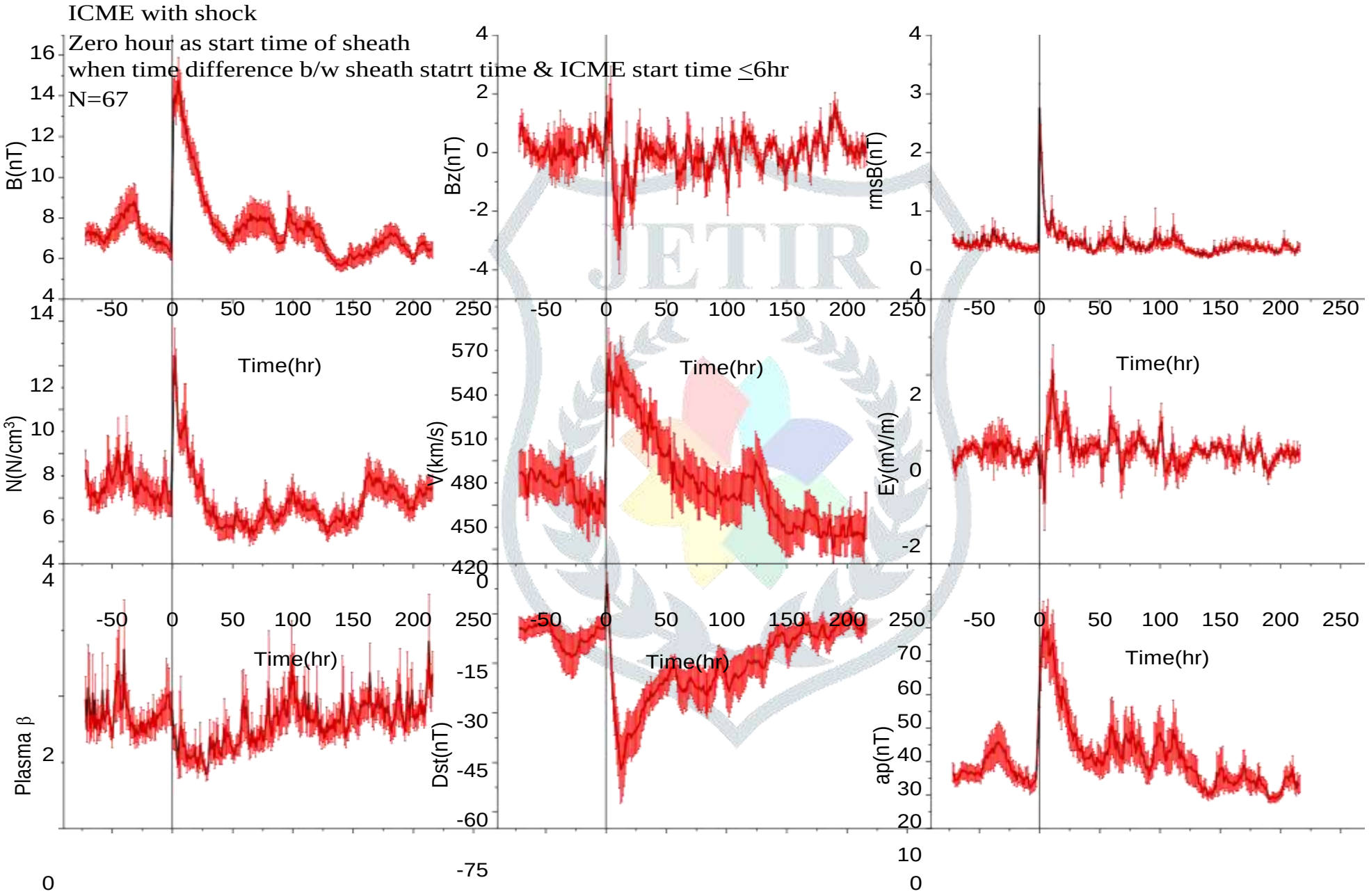
ICME with shock
Zero hour as start time of sheath
when time difference b/w sheath statrt time & ICME start time ≤6hr
N=67
B(nT)
Bz(nT)
rmsB(nT)
N(N/cm3)
V(km/s)
Ey(mV/m)
Plasma β
Dst(nT)
ap(nT)
Time(hr)

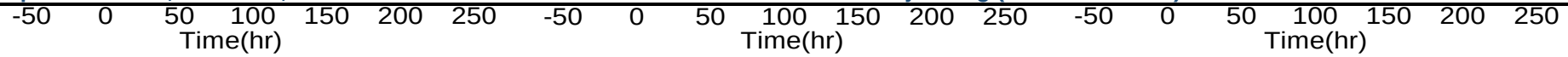

Fig.3a. Superposed epoch analysis results of hourly data for various parameters with respect to the arrival of the sheath when start time of ICMEs and sheath start time gap ≤6hr with shock.

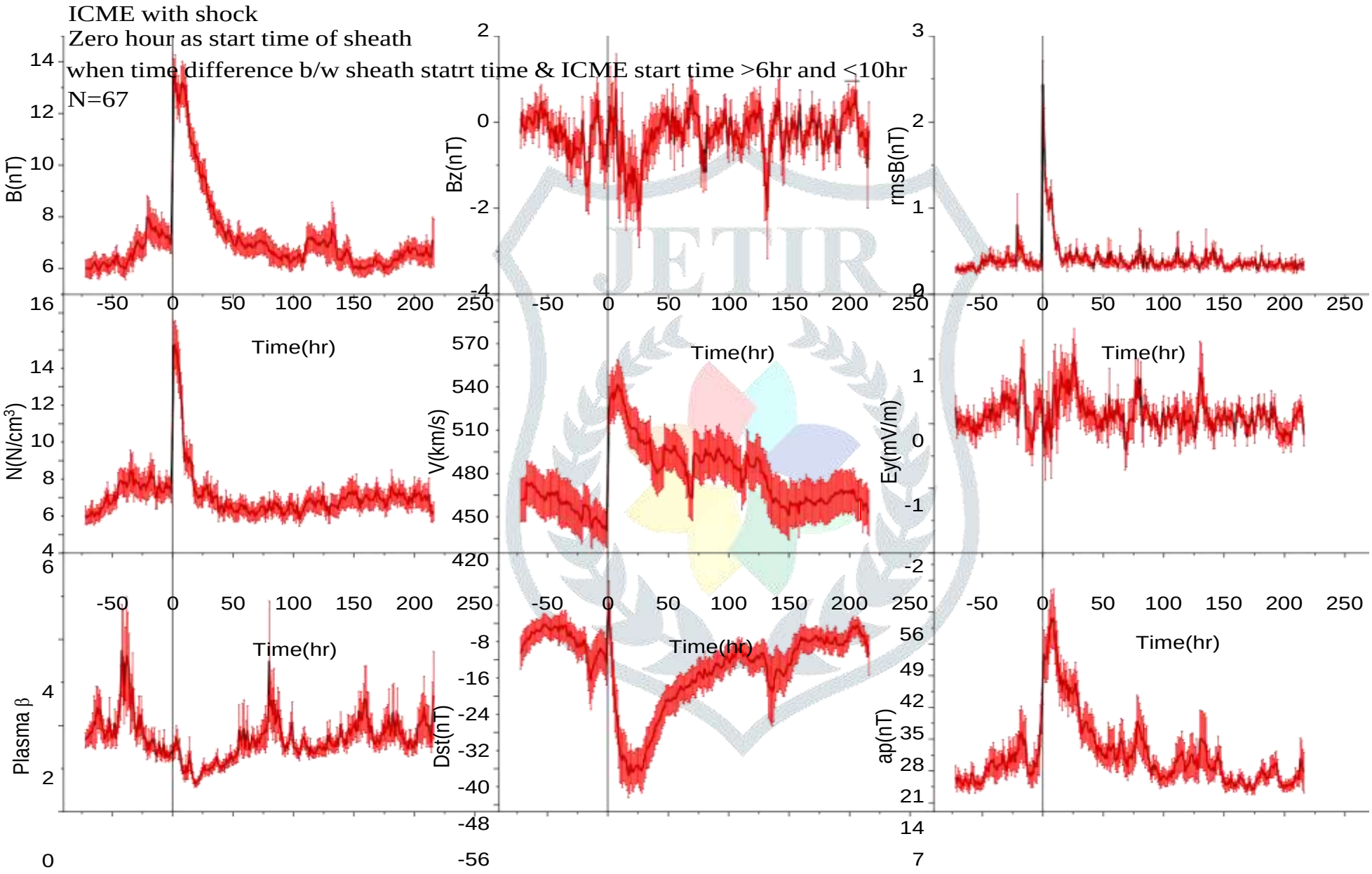
ICME with shock
Zero hour as start time of sheath
when time difference b/w sheath statrt time & ICME start time >6hr and <10hr
N=67
B(nT)
Bz(nT)
rmsB(nT)
N(N/cm3)
V(km/s)
Ey(mV/m)
Plasma β
Dst(nT)
ap(nT)
Time(hr)

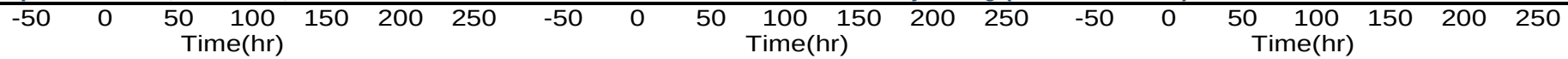

Fig.3b. Superposed epoch analysis results of hourly data for various parameters with respect to the arrival of the sheath when start time of ICMEs and sheath start time gap .6hr and ≤10hr with shock.

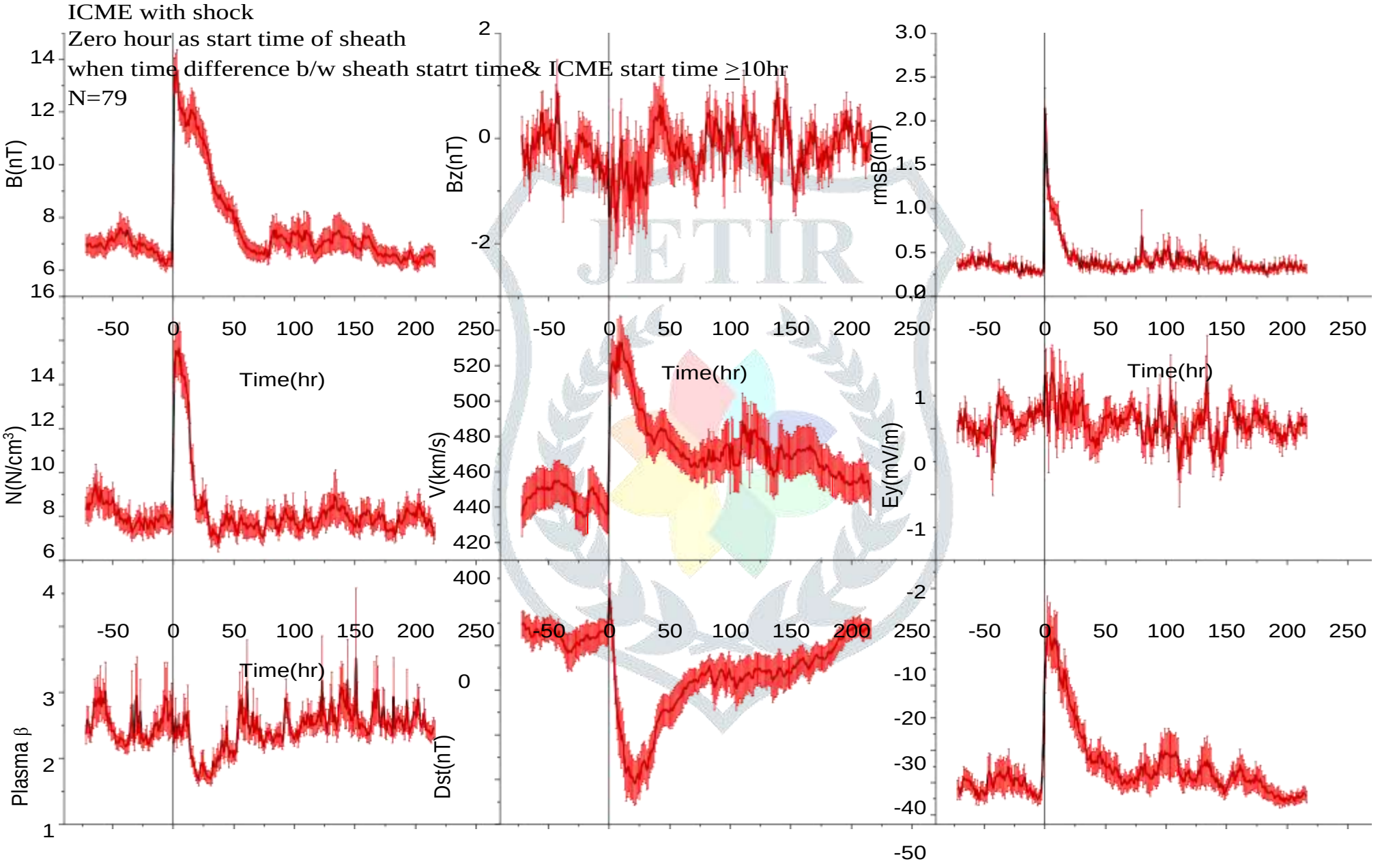
ICME with shock
Zero hour as start time of sheath
when time difference b/w sheath statrt time& ICME start time ≥10hr
N=79
B(nT)
Bz(nT)
rmsB(nT)
N(N/cm3)
V(km/s)
Ey(mV/m)
Plasma β
Dst(nT)
Time(hr)
Time(hr)
Time(hr)
Time(hr)

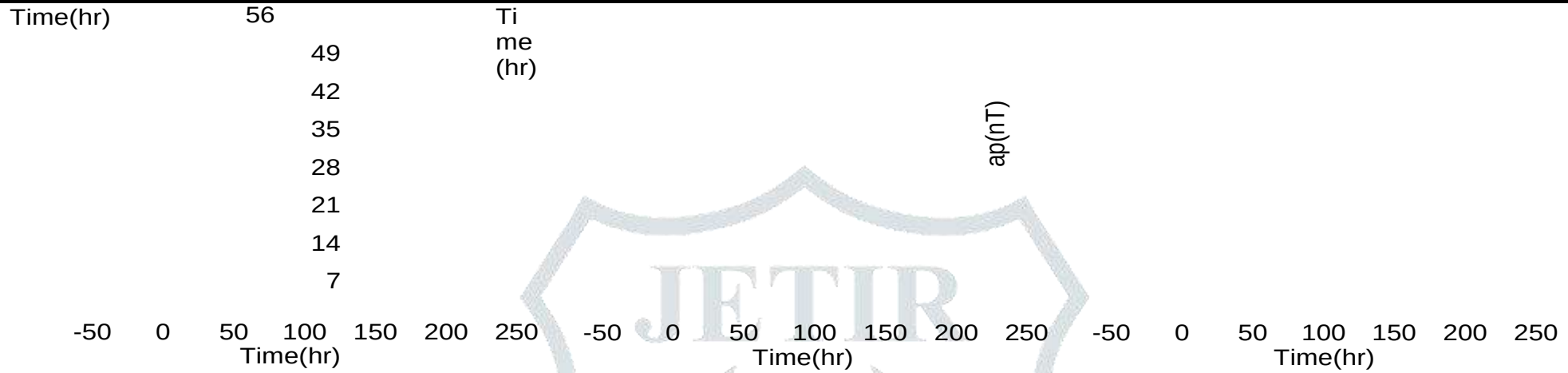

Fig.3c. Superposed epoch analysis results of hourly data for various parameters with respect to the arrival of the sheath when start time of ICMEs and sheath start time gap ≥10hr with shock.

Table 4a:Correlation coefficients between plasma parameters and ap-index on the bases of superposed results Main phase(R1) and Recovery phase(R2) for all groups of ICME with sheath (sheath start time / ICME start time as zero hour) associated with shocks/ no shocks for the different phase of solar cycle

Group	No. of events	B(nT)		Bz(nT)		rmsB(nT)		N(N/cm^3)		V(km/s)		Ey(mV/m)		Plasma Betta		Dst(nT)	
		R1	R2	R1	R2	R1	R2	R1	R2	R1	R2	R1	R2	R1	R2	R1	R2
ICME without shock	112	-*	0.45	-*	-0.16	-*	0.64	-*	0.41	-*	0.15	-*	0.12	-*	-0.35	-*	-0.44
ICME with Shock	213	-*	0.965	-*	-0.75	-*	0.71	-*	0.54	-*	0.93	-*	0.74	-*	-0.78	-*	-0.88
Sheath without shock	112	0.91	0.71	-0.08	0.07	-0.86	0.49	-0.42	0.53	0.88	0.02	-0.03	-0.10	-0.76	-0.56	-0.62	-0.63
Sheath with shock	213	0.80	0.96	-0.21	-0.71	-0.94	0.87	0.62	0.67	0.84	0.93	0.19	0.71	-0.55	-0.69	-0.71	-0.87
Group Sheath without shock																	
G-1	60	-0.34	0.67	-0.42	-0.08	0.35	0.57	0.28	0.34	0.67	-0.11	0.49	-0.12	0.31	-0.06	0.40	-0.59
G-2	21	0.93	0.74	0.03	-0.17	-0.05	0.53	0.02	0.59	0.83	-0.20	-0.20	0.17	-0.75	0.08	-0.90	-0.57
G-3	31	-0.82	0.65	-0.07	-0.56	-0.14	0.43	-0.24	0.20	0.62	0.48	0.23	0.50	-0.14	-0.16	-0.70	-0.70
Group Sheath with shock																	
G-1	67	-0.06	-0.84	0.88	0.52	0.84	-0.51	0.46	0.01	-0.16	-0.91	-0.821	-0.50	0.33	0.65	-0.35	-0.90
G-2	67	0.64	-0.87	0.64	0.45	0.94	-0.39	0.95	-0.06	-0.00	-0.72	-0.71	-0.51	0.77	0.67	0.18	-0.90
G-3	79	0.26	-0.91	-0.27	0.24	0.94	-0.21	0.62	0.11	-0.42	-0.81	0.26	-0.18	0.47	0.64	0.67	-0.88

-* very short duration for main phase (only few hours)

Table 4b: Correlation coefficients between plasma parameters and Dst index on the bases of superposed results Main phase(R1) and Recovery phase(R2) for all groups of ICME with sheath (sheath start time / ICME start time as zero hour) associated with shocks/ no shocks for the different phase of solar cycle

Group	No. of events	B(nT)		Bz(nT)		rmsB(nT)		N(N/cm^3)		V(km/s)		Ey(mV/m)		Plasma Betta		ap(nT)	
		R1	R2	R1	R2	R1	R2	R1	R2	R1	R2	R1	R2	R1	R2	R1	R2
ICME without shock	112	-0.33	-0.67	-0.46	-0.10	0.83	-0.36	0.92	-0.56	0.69	0.09	0.44	0.07	0.80	0.47	0.74	-0.49
ICME with Shock	213	0.81	-0.90	0.88	0.49	0.84	-0.57	0.93	0.17	0.71	-0.97	-0.81	-0.55	0.88	0.85	0.94	-0.94
Sheath without shock	112	-0.62	-0.82	-0.777	-0.31	0.91	-0.36	0.89	-0.61	0.34	0.13	0.75	0.32	0.83	0.56	0.31	-0.61
Sheath with shock	213	0.14	-0.89	0.70	0.59	0.85	-0.65	0.68	-0.17	0.49	-0.94	-0.78	-0.58	0.83	0.85	-0.35	-0.93
Group Sheath without shock																	
G-1	60	-0.94	-0.62	-0.76	-0.14	0.94	-0.38	0.91	-0.40	0.72	0.14	0.73	0.24	0.91	0.35	0.72	-0.61
G-2	21	0.47	-0.63	-0.06	0.17	0.70	-0.16	0.74	-0.16	0.67	-0.08	-0.08	-0.18	0.64	0.01	0.26	-0.59
G-3	31	0.69	-058	0.36	0.42	0.35	-0.04	0.47	0.11	0.13	-0.30	-0.37	-0.30	-0.42	0.34	-0.20	-0.71
Group Sheath with shock																	
G-1	67	-*	0.95	-*	-0.54	-*	0.82	-*	0.58	-*	0.82	-*	0.49	-*	-0.49	-*	-0.76
G-2	67	-0.69	0.94	-0.10	-0.55	-0.43	0.66	-0.96	0.61	0.19	0.83	0.31	0.57	-0.44	-0.600	-0.80	-0.85
G-3	79	-*	0.95	-*	-0.50	-*	0.84	-*	0.82	-*	0.92	-*	0.44	-*	-0.37	-*	-0.63

-* very short duration for main phase (only few hours)

3. Statistical study of ICMEs/sheaths when associated with shocks and no shocks

In order to compare the geomagnetic response of ICMEs/ Sheath we use the statistical study correlation analysis in this study, we do the correlation analysis between Dst/ap index and plasma field parameters during the main phase as well as the recovery phase for ICMEs/sheath associated or not associated with shocks. Table 4a and 4b represent the results of correlation analysis ap and Dst index respectively. All the parameters show a good correlation with ap index during the passage of ICMEs with a sheath with shocks during the recovery phase. In case of the Dst index, we get good correlations between plasma/ field parameters for both the main phase as well as recovery phase especially when ICMEs/sheath are associated with shocks. However, in the groups, G1, G2 and G3 Dst and ap index show the best correlation with B, rmsB, V and Ey during the recovery phase when associated with shocks.

Conclusion

From the analysis performed, we conclude the following.

- When ICMEs are associated with sheath are more geoeffective.
- Shocks, when associated with ICMEs/ sheath, are more geoeffective than not associated with shocks.
- Geomagnetic disturbance with Dst and Ap amplitude is best correlated with the magnetic field, plasma velocity and down dusk electric field during the recovery phase for all the groups of ICMEs and sheath.
- The recovery time for the geomagnetic storms (Dst or Ap) is lower for ICMEs/sheath without shocks. In other words when shocks associated with streams represent a clear picture of correlation with storms.
- In case of G1 group i.e., when ICME with sheath (start time gap<6h) with shocks formed the best correlation with Dst as well as Ap for All parameters except density in comparison of other groups.

Acknowledgements

This work was funded by the Government of India Ministry of Science& Technology Department of Science & Technology KIRAN DIVISION. Therefore, we acknowledge and thank DST for its financial support. We appreciate the continuous support of the Centre for Theoretical Physics, JMI, and Prof. Sushant G. Ghosh.

We appreciate the publication of ICMEs Catalogue by I.G. Richardson & H.V. Cane and Jian. We acknowledge the use of the OmniWeb database of NASA/GSFC also.

References

[1] Badruddin, Hassan Basurah, M. Yengui, 2017. Study of the geoeffectiveness of interplanetary magnetic clouds. Planetary and Space Science, 139, 1-10, http://dx.doi.org/10.1016/j.pss.2017.03.001
[2] Borrini, G., Gosling, J.T., Bame, S.J., Feldman, W.C., 1982. Helium abundance enhancements in the solar wind. J. Geophys. Res., 87, 7370.
[3] Bothmer, V., Schwenn, R., 1998. The structure and origin of magnetic clouds in the solar wind, Ann. Geophys., 16, 1.
[4] Burlaga, L.F., Sittle E., Mariani, F., Schwenn, R., 1981. Magnetic loop behind an interplanetary shock: Voyager, Helios, and IMP 8 observations, J. Geohpys. Res., 86, 6673
[5] Crooker, N.U., 2000. Solar and heliospheric geoeffective disturbances, J. Atmos. Solar-Terr. Phys. 62, 1071.
[6] Ebert, A. D. Junying Yu, Ferrill F. Rose Jr, Virginia B. Mattis, Christian L. Lorson, James A. Thomson and Clive N. Svendsen, 2009. Induced pluripotent stem cells from a spinal muscular atrophy patient, *Nature*, 457, 277–280.
[7] Galvin, A.B., Ipavich, F.M., Gloeckler, G., Hovestadt, D., Bame, S.J., Klecker, B., Scholer, M., Tsurutani, B.T., 1987. Solar wind iron charge states preceding a driver plasma, J. Geophys. Res., 92, 12069**.**
[8] Goldstein, R., Neugebauer, M., and Clay D., 1998. A statistical study of coronal mass ejection plasma flows, J. Geophys. Res., 4761-4766.
[9] Gopalswamy, N., Akiyama, S., Yashiro, S., Michalek, G., Lepping, R.P., 2008. Solar sources and geospace consequences of interplanetary magnetic clouds observed during solar cycle 23, J. Atmos. Sol-Terr. Phys., 70, 245
[10] Gosling, J.T., 1990. Physics of Magnetic Flux Ropes, Geographical Monograph Series, 58, AUG, Washington DC, 343
[11] Gosling, J.T., 1993. The solar flare myth, J. Geophys. Res., 98, 18937.
[12] Gonzalez, W.D., Tsurutani, B.T., Clua de Gonzalez, A.L., 1999. Interplanetary origin of geomagnetic storms, Space Sci. Rev., 88, 529.
[13] Guo, J., Feng, X., Zhang, J., Zuo, P., Xiang, C., 2010. Statistical properties and geoefficiency of interplanetary coronal mass ejections and their sheaths during intense geomagnetic storms, J. Geophys. Res.,115, 9107.
[14] Huttunen, K.E.J., Schwenn, R., Bothmer, V., Koskinen, H.E.J., 2005. Properties and geoeffectiveness of magnetic clouds in the rising, maximum and early declining phases of solar cycle 23, Ann. Geophys. 23, 625
[15] Jian, L., Russel, C.T., Luhmann, J.G., Skoug, R.M., 2006a. Properties of Interplanetary Coronal Mass Ejections at One AU During 1995-2004, Sol. Phys. 239, 393
[16] Jian, L., Russel, C.T., Luhmann, J.G., Skoug, R.M., 2006b. Properties of Stream Interactions at One AU During 1995-2004, Sol. Phys. 239, 337
[17] Kilpua, E.K.J., Lee, C.O., Luhmann, J.G., Li, Y., 2011. Interplanetary coronal mass ejections in the near-Earth solar wind during the minimum periods following solar cycles 22 and 23, Ann. Geophys., 29, 1455

[18] Kilpua, Emilia;Koskinen, Hannu E. J., Pulkkinen, Tuija I., 2017.Coronal mass ejections and their sheath regions in interplanetary space, Living Reviews in Solar Physics, 14, 1, 83.

[19] Klein, L.W., Burlaga, L.F., 1982. Interplanetary magnetic clouds at 1 AU, J. Geophys. Res., 87, 613.
[20] Lindsay, G.M., Luhmann, J.G., Russell, C.T., Gosling, J.T., 1999. Relationships between coronal mass ejection speeds from coronagraph images and interplanetary characteristics of associated interplanetary coronal mass ejections, J. Geophys. Res. 104, 12515.
[21] Liu, Y., Richardson, J.D., Belcher, J.W., 2005. A statistical study of the properties of interplanetary coronal mass ejections from 0.3 to 5.4 AU, Planet. Space Sci., 53, 3.
[22] Mitsakou, E., Babasidis, G., Moussas, X., 2009. Interplanetary coronal mass ejections during the descending cycle 23: Sheath and ejecta properties comparison, Adv. Space Res., 43, 495.

[23] Mustajab F. and Badruddin, 2013. Relative geo-effectiveness of coronal mass ejections with distinct features in interplanetary space, Planetary and Space Science, 82, 43-61.

[24] Mustajab F. and Badruddin, 2017. Passage of the high-speed solar wind streams, their plasma/field properties, and resulting geomagnetic disturbances, Advances in Space Research, 60, 1, 144-152

[25] Mustajab,F., Badruddin, B., Asiri H., 2019. Study of the relative geoeffectiveness of high-speed solar wind streams of different speed and different durations, Advances in Space Research, 64, 9, 1740-1750

[26] Richardson, I.G., Cane, H.V., 1993. Signatures of shock drivers in the solar wind and their dependence on the solar source location, J. Geophys. Res. 98, 15295.
[27] Richardson, I.G., Cane, H.V., 2005. Near-Earth interplanetary coronal mass ejections during solar cycle 23 (1996 – 2009): Catalog and summary of properties, Solar Phys., 264, 189–237.
[28] Richardson, I.G., Cane, H.V., 2010. Near-Earth interplanetary coronal mass ejections during solar cycle 23 (1996 - 2009): Catalog and Summary of Properties, Solar Phys., 264, 189
[29] Russell, C.T., Shinde, A.A., 2003. ICME Identification from Solar Wind Ion Measurements, Solar Phys., 216, 285
[30] Schwenn, R., dal Lago, A., Huttunen, E., Gonzalez, W.D., 2005. The association of coronal mass ejections with their effects near the Earth, Ann. Geophys. 23, 1033.
[31] Tsurutani, B.T., Gonzalez, W.D., Tang, F., Akasofu, S.I., Smith, E.J., 1988. Origin of interplanetary southward magnetic fields responsible for major magnetic storms near solar maximum (1978-1979), J. Geophys. Res., 93, 8519.
[32] Wang, C., Du, D., Richardson, J.D., 2005. Characteristics of the interplanetary coronal mass ejections in the heliosphere between 0.3 and 5.4 AU, J. Geophys. Res., 110, 10107.
[33] Wei, F.S., Liu, R., Fan, Q.L., Feng, X.S., 2003. Identification of the magnetic cloud boundary layers, J. Geophys. Res., 108, 1263.
[34] Wimmer-Schweingruber, R.F., Crooker, N.U., Balogh, A., Bothmer, V., Forsyth, R.J., Gazis, P., et al., 2006. Understanding Interplanetary Coronal Mass Ejection Signatures, Space Sci. Rev., 123, 177.
[35] Zurbuchen, T.H., Richardson, I.G., 2006. In-Situ Solar Wind and Magnetic Field Signatures of Interplanetary Coronal Mass Ejections, Space Sci. Rev., 123, 31.